

Connection between Neutral Pion Decay and Proton Compton Scattering

MAURICE JACOB† AND JON MATHEWS

Norman Bridge Laboratory of Physics, California Institute of Technology, Pasadena, California

(Received August 20, 1959)

The inclusion of the single-pion intermediate state significantly improves the agreement between theory and experiment for proton Compton scattering. Excitation functions and angular distributions for various assumed values of the π^0 lifetime are presented. On this basis one may definitely exclude π^0 lifetimes $>10^{-16}$ sec or $<5 \times 10^{-19}$ sec.

RECENTLY several proposals have been made to study the singularities in matrix elements produced by single-particle intermediate states.¹ Such intermediate states are associated with poles in the overall matrix element, the denominator having the form $q^2 - \mu^2$ with q the four-momentum transferred by the intermediate particle (of mass μ). The residue is the product of the matrix elements associated with the two "pieces" into which the process is divided by "cutting" the single-particle line. In general, the pole will be located at an unphysical scattering angle for the overall process, but in favorable cases the pole may be sufficiently "near" the physical region that an extrapolation procedure will determine the residue at the pole.

In this paper we are concerned with the existence of such a one-particle state in certain matrix elements for proton Compton scattering. Namely, in matrix elements of the form indicated in Fig. 1, the process $\gamma + p \rightarrow \gamma + p$ may be decomposed into the two simpler processes $\pi^0 \rightarrow 2\gamma$ and $p \rightarrow p + \pi^0$. The residue of the pole will be the product of the (renormalized) pion-nucleon coupling constant and the matrix element for the two-photon decay of the π^0 .² More specifically, the center-of-mass (c.m.) differential cross section will be of the form

$$\left(\frac{4\pi M}{e^2}\right)^2 \frac{d\sigma}{d\Omega} = \frac{2}{\mu\tau} \left(\frac{4\pi}{e^2}\right)^2 \left(\frac{g^2}{4\pi}\right) \left(\frac{k}{E}\right)^2 \left(\frac{M}{\mu}\right)^2 \frac{(1-y)^3}{(y-y_0)^2} + \frac{F(k,y)}{y-y_0}, \quad (1)$$

where $F(k,y)$ is finite at $y=y_0 \equiv 1 + (\mu^2/2k^2)$. In our notation μ is the neutral pion mass, M is the proton mass, e is the rationalized electronic charge ($e^2/4\pi \approx 1/137$), g is the rationalized pion-nucleon coupling constant, k is the c.m. photon energy, E is the total c.m. energy, y is the cosine of the c.m. scattering angle, and τ is the lifetime of the neutral pion. We use units such that \hbar and c are one; $(e^2/4\pi M)^2$ is then a natural unit for Compton cross sections, equal to 2.36×10^{-32} cm².

In principle, we could determine τ from an experi-

mental angular distribution at a fixed c.m. energy, by fitting the observed data to a function such as³

$$\frac{d\sigma}{d\Omega} = \frac{A(1-y)^3}{(y-y_0)^2} + (B+Cy+Dy^2)(y-y_0)^{-1}, \quad (2)$$

where A, B, C, D are constants. The value of A would then, by comparison with (1), yield the pion lifetime τ . In fact, however, present experimental data on Compton angular distributions is very crude, and cannot be used to determine the parameter A of (2).

It seems clear that experiments of quite high accuracy will have to be done if this method is to yield a useful result. At low energies the residue of the pole is small because of the factor k^2 in (1). At high energies the pole is very near $y=1$, while the effect vanishes at $y=1$, because of the factor $(1-y)^3$ in (1). However, there seems to be no reason in principle why this extrapolation technique could not be applied to a precise angular distribution at a c.m. energy $k \sim \mu$, to yield a value for τ .

In this note we have adopted a different procedure, less rigorous than the one outlined above but quite capable, we believe, of yielding useful information on the π^0 lifetime when applied to presently existing experimental data.⁴⁻⁶ We have simply added the matrix element of Fig. 1 to dispersion-theoretic estimates of proton Compton amplitudes⁷ which neglected such contributions, and compared the resulting predictions with

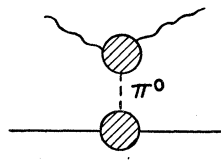


FIG. 1. Intermediate neutral pion in proton Compton scattering.

³ We are ignoring another pole, arising from the single nucleon intermediate state in the crossed Born approximation diagram (as in Fig. 2). This pole occurs at $y = -2E_k/k$, which is far removed from the physical region at the energies considered in this paper. If the precision of the calculations warranted it, a term representing this pole (with residue e^2) could easily be added to the right-hand side of Eq. (2).

⁴ Pugh, Gomez, Frisch, and Janes, *Phys. Rev.* **105**, 982 (1957).
⁵ T. Yamagata, Ph.D. thesis, University of Illinois, 1956 (unpublished); Yamagata, Auerbach, Bernardini, Filosofo, Hanson, and Odian, *Bull. Am. Phys. Soc.* **1**, 383 (1956).

⁶ A. Odian, private communication to R. Gomez, 1959.
⁷ J. Mathews, Ph.D. thesis, California Institute of Technology, 1957 (unpublished); J. Mathews and M. Gell-Mann, *Bull. Am. Phys. Soc.* **2**, 392 (1957).

† On a French "Commissariat à l'Energie Atomique" Fellowship.

¹ G. F. Chew, *Phys. Rev.* **112**, 1380 (1958); G. F. Chew, *Bull. Am. Phys. Soc.* **3**, 417 (1958); Taylor, Moravcsik, and Uretsky, *Phys. Rev.* **113**, 689 (1959).

² We shall neglect modes of π^0 decay other than $\pi^0 \rightarrow 2\gamma$.

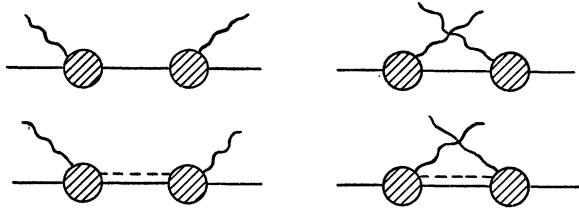


FIG. 2. Intermediate states considered in dispersion theory of reference 7.

the experimental data. We have assumed $g^2/4\pi = 0.082(2M/\mu_+)^2$, where μ_+ is the mass of the charged pion. Some of the details are outlined in the Appendix.

There are three principal assumptions involved in this program. In the first place, we are now considering the π^0 decay "black box" of Fig. 1 with the π^0 off the mass shell, so that the matrix element need not have the same value as it does for π^0 decay. We do not feel that the dependence of this form factor on the mass of the virtual pion is important at the low energies at which we are working, however, since the pion decay presumably involves nucleon pair formation and the characteristic energies tend to be of the order of the nucleon rest mass, rather than the pion rest mass.

In the second place, the other black box of Fig. 1 is also being evaluated for virtual pions with the wrong mass, so that we should include the form factor associated with the pion-nucleon coupling constant g . Here we are on very uncertain ground, since there is no experimental information on the momentum-dependence of this form factor. We shall simply assume that the interaction does not vary significantly for momentum transfers of the order of one or two pion masses. This result may be "deduced" from the work of Goldberger and Treiman,⁸ but these authors essentially forced their result by considering only the nucleon-antinucleon intermediate state in their dispersion-theoretic calculations.

Finally, there is the possibility that other intermediate states, besides the one-pion state, may make important contributions. Most of these contributions have certainly been included in the dispersion-theoretic amplitudes,⁷ which consider the nucleon and nucleon-plus-pion intermediate states of Fig. 2. However, certain points are confusing; for example, the Feynman diagram of Fig. 3 does not appear to be included in Fig. 2.⁹ We shall simply assume that the extra contribu-

FIG. 3. "Seagull" diagram in Compton scattering



⁸ M. L. Goldberger and S. B. Treiman, Phys. Rev. **110**, 1178 (1958).

⁹ This difficulty underlies the disagreement between the Compton scattering calculations of Karzas, Watson, and Zachariasen, Phys. Rev. **110**, 253 (1958), and our dispersion-theory predictions. A significant fraction of their amplitude [their $A_s(k)$] results from the static analogy of our Fig. 3.

tion (if any) from such terms are not important at energies $k \leq 2\mu$.

In this connection, it is of some interest to consider the location of the branch line singularity nearest to the pole at $y=y_0$. This branch line is given by $y > y_b \equiv 1 + 2\mu^2/k^2$. If we use Chew's criterion¹ for extrapolation, namely that only those values of y for which

$$|y - y_0| < |y_0 - y_b|, \quad (3)$$

are acceptable for extrapolation, then the "useful region" (3) consists of $-0.21 < y < 1$ at $k=140$ Mev and $0.29 < y < 1$ at $k=190$ Mev.

The principal experimental results on proton Compton scattering consists of excitation functions at

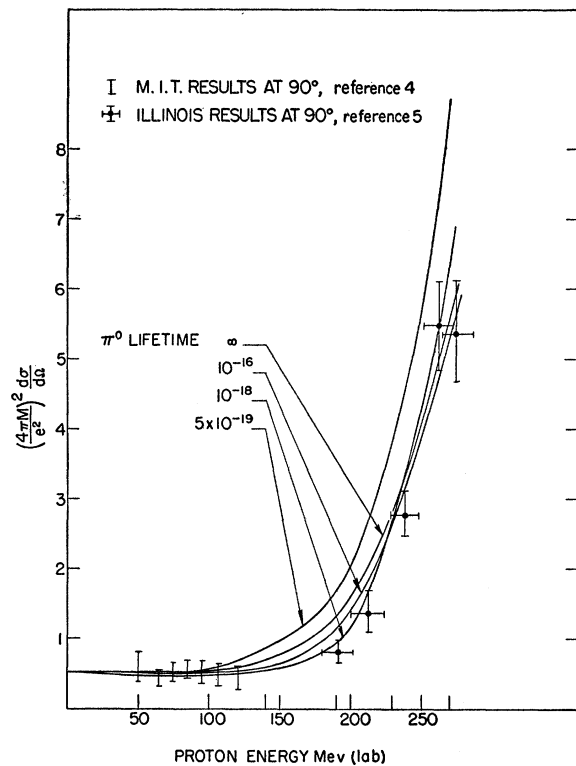


FIG. 4. Theoretical excitation functions at $\theta_{e.m.} = 90^\circ$, for various π^0 lifetimes, and experimental data.

$\theta_{e.m.} = 90^\circ$ and $\theta_{e.m.} = 135^\circ$, at lab photon energies up to about 300 Mev. In Figs. 4 and 5 we have plotted theoretical excitation functions for various assumed pion lifetimes. It seems clear that omission of the pion-decay matrix element of Fig. 1 ($\tau = \infty$ in Figs. 4 and 5) causes significant disagreement with experiment. In fact, both Fig. 4 and Fig. 5 clearly indicate that $\tau > 10^{-16}$ sec and $\tau < 5 \times 10^{-19}$ sec are excluded. At all energies and angles which we considered, the effect of gradually "turning on" the π^0 decay was to lower slowly, and then, for $\tau < 3 \times 10^{-18}$ sec to raise rapidly the predicted differential cross sections. This behavior is illustrated in Fig. 6, where $d\sigma/d\Omega$ at lab photon

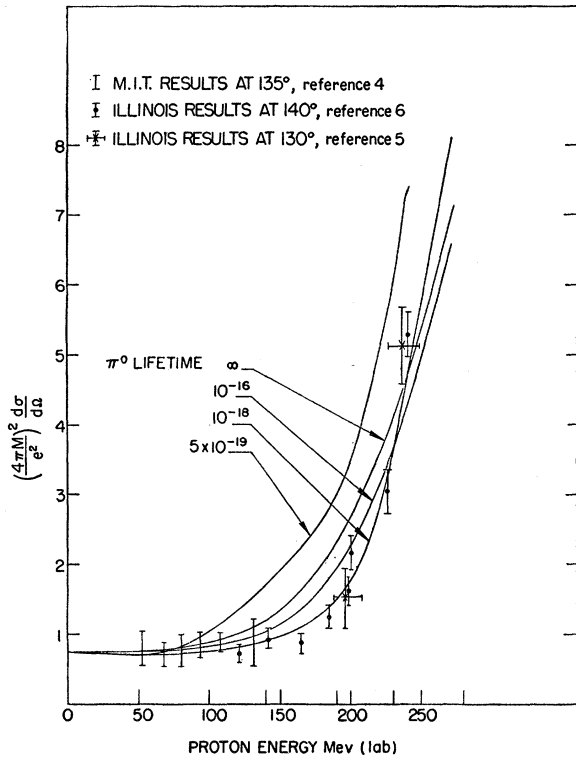


FIG. 5. Theoretical excitation functions at $\theta_{c.m.} = 135^\circ$, for various π^0 lifetimes, and experimental data.

energies of 140 Mev and 190 Mev, and c.m. angles of 90° and 135° , is plotted against the assumed π^0 lifetimes. The shaded regions indicate approximately the uncertainties in the experimental cross sections.

We feel that the data at energies in the 150–200 Mev range are the most useful. At lower energies the data are too insensitive to τ and at higher energies theoretical uncertainties arise. Angular distributions for various energies and π^0 lifetimes are given in Figs. 7 and 8. We have also computed the polarization P of the recoil proton. The product $P d\sigma/d\Omega$ turns out not to depend on τ ; at 190 Mev and with $\tau = 10^{-17}$ sec (say) $P \sim 45\%$ at 90° and $P \sim 30\%$ at 135° , the positive direction being along $\mathbf{k} \times \mathbf{k}'$, where \mathbf{k} and \mathbf{k}' are unit vectors along the photon initial and final momenta.

Since the result depends explicitly on the value of the pion nucleon coupling constant we compare the results of assuming $g^2/4\pi = 0.078(2M/\mu_+)^2$ in many of

TABLE I. Effect of the value of $g^2/4\pi$ on $d\sigma/d\Omega$.

Incident photon energies (Mev)	50	100	140	190	230	270
$(4\pi M/e^2)^2 d\sigma/d\Omega$ with $g^2/4\pi = 0.078(2M/\mu_+)^2$	0.467	0.461	0.504	0.947	2.67	6.32
$(4\pi M/e^2)^2 d\sigma/d\Omega$ with $g^2/4\pi = 0.082(2M/\mu_+)^2$	0.467	0.464	0.517	0.974	2.72	6.42

our calculations. The difference was almost negligible for the purposes of this paper. In Table I we indicate the effect on $d\sigma/d\Omega$ at $\theta_{c.m.} = 90^\circ$ for $\tau = 10^{-18}$ sec.

The dispersion-theoretic Compton amplitudes were based on experimental single-pion photoproduction cross sections. At low energies (≤ 300 Mev) pion photoproduction may fairly accurately be assumed to result from two amplitudes alone; a charged $E1(\frac{1}{2})$ amplitude and an $M1(\frac{3}{2})$ amplitude in the $T = \frac{3}{2}$ state. Since there are then only two energy dependent amplitudes they may be expressed as functions of the total cross sections for π^0 and π^+ photoproduction.¹⁰ In the original calculations,⁷ this multipole analysis was assumed to remain valid for all photon energies; since the dispersion

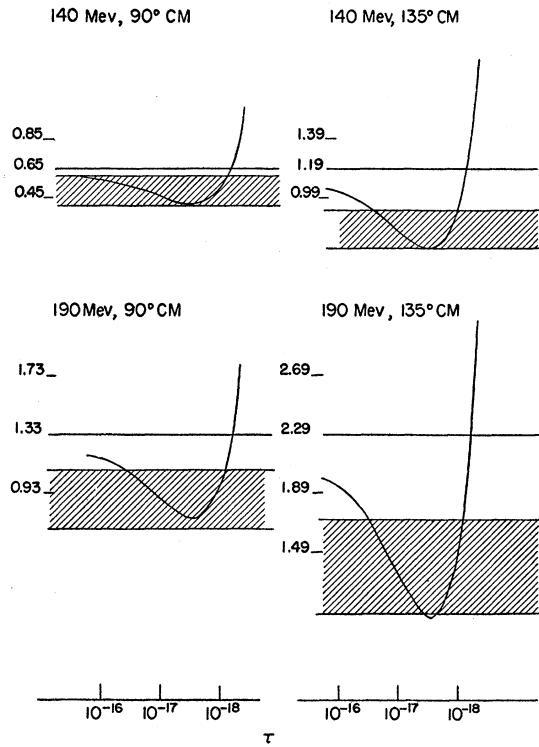


FIG. 6. Several differential cross sections, plotted as function of π^0 lifetime.

integrals converge rapidly and contributions from beyond 350 Mev are quite small, it was felt that a negligible error was involved in this approximation. In order to test the sensitivity of the results of our present paper to this assumption, which we shall call (a), we have considered a second assumption (b), which considers photoproduction below 500 Mev to proceed through the above-mentioned amplitudes, while above 500 Mev the only contributing amplitudes are independent charged and neutral $E1(\frac{3}{2})$ amplitudes.¹¹ Again

¹⁰ In the dispersion calculation, only the magnitudes of the photoproduction matrix elements enter, not their phases.

¹¹ R. F. Peierls, Phys. Rev. Letters 1, 174 (1958).

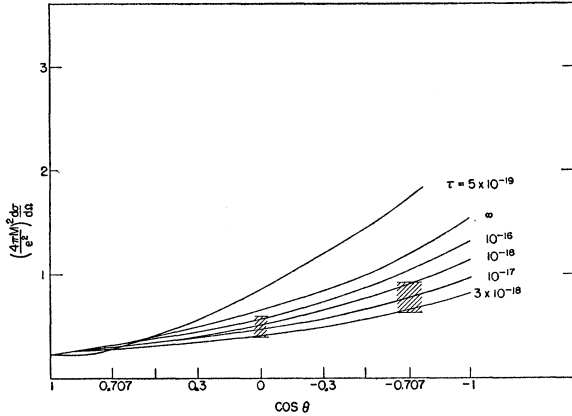


FIG. 7. Theoretical angular distributions at 140 Mev.

the total photomeson cross sections suffice as input data, and, as expected, the results differ only slightly from those arrived at by assumption (a). In all of the graphs we have used assumption (b); in Table II we compare the Compton scattering cross section at $\theta_{c.m.} = 90^\circ$, $\tau = 10^{-18}$ sec, resulting from the two assumptions. It is felt that the difference shown is a reasonable estimate of the error introduced by our approximate photo-production analysis.

Dispersion-theoretic results for the Compton scattering amplitude, based on assumptions (a) and (b) are given in the Appendix.

In conclusion, we see that the existence of the 2γ electromagnetic decay mode of the neutral pion can certainly be observed in existing proton Compton scattering data. Furthermore, certain extreme values for the lifetime, such as 10^{-16} sec on the upper side and 5×10^{-19} sec on the lower side, can be excluded. It would appear *a priori* that one should be able to establish limits which differ by a factor of less than 200. The setting of more precise limits by considerations of this type is difficult because of the insensitivity of $d\sigma/d\Omega$ to the variations in τ (Fig. 6). It seemed of some interest,

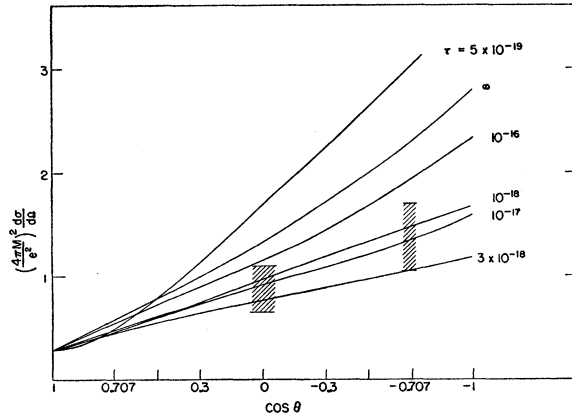


FIG. 8. Theoretical angular distributions at 190 Mev.

however, to point out that existing experimental data on proton Compton scattering suggest as definite a value for the π^0 lifetime as any other current approach, theoretical or experimental.¹²

Since the completion of this work, our attention has been called to a preprint on this subject by F. E. Low, and also the work of L. G. Hyman *et al.*¹³ Their conclusions in general agree with the results of this paper.

 TABLE II. The value of $d\sigma/d\Omega$ for assumptions (a) and (b).

Incident photon energies (Mev)	50	100	140	190	230	270
$(4\pi M/e^2)^2 d\sigma/d\Omega$ with assumption (a)	0.470	0.473	0.528	0.981	2.67	6.16
$(4\pi M/e^2)^2 d\sigma/d\Omega$ with assumption (b)	0.467	0.464	0.517	0.974	2.72	6.42

APPENDIX

In the c.m. system the R matrix for Compton scattering may be written in the form:

$$\begin{aligned}
 R = & g_1(k, y) \hat{e} \cdot \hat{e} + g_2(k, y) \hat{e} \cdot \hat{k}' \hat{e}' \cdot \hat{k} + g_3(k, y) i\sigma \cdot \hat{e} \times \hat{e}' \\
 & + g_4(k, y) \hat{e} \cdot \hat{e}' i\sigma \cdot \hat{k} \times \hat{k}' + g_5(k, y) \\
 & \times i\sigma (\hat{e} \cdot \hat{k}' \hat{e}' \times \hat{k} - \hat{e}' \cdot \hat{k} \hat{e} \times \hat{k}') \\
 & + g_6(k, y) i\sigma \cdot (\hat{e} \cdot \hat{k}' \hat{e}' \times \hat{k}' - \hat{e}' \cdot \hat{k} \hat{e} \times \hat{k}),
 \end{aligned}$$

\hat{e} and \hat{e}' are the initial and final polarization unit vectors; \hat{k} and \hat{k}' are unit vectors along the initial and final photon momenta. The differential cross section is

$$\begin{aligned}
 d\sigma/d\Omega = & (kE_k/2\pi E)^2 \left[\frac{1}{2} |g_1|^2 (1+y^2) + \frac{1}{2} |g_2|^2 (1-y^2)^2 \right. \\
 & + (-\text{Reg}_1^* g_2 + \text{Reg}_3^* g_4 + 6 \text{Reg}_5^* g_6 - 2 \text{Reg}_3^* g_5 \\
 & - 2 \text{Reg}_4^* g_6) y (1-y^2) - 2 \text{Reg}_4^* g_6 y^2 (1-y^2) \\
 & + |g_5|^2 (1-y^2) (1+2y^2) + \frac{1}{2} |g_3|^2 (3-y^2) \\
 & \left. + \frac{1}{2} |g_4|^2 (1-y^4) + (3 |g_6|^2 - 4 \text{Reg}_3^* g_6) (1-y^2) \right],
 \end{aligned}$$

E_k is the proton c.m. energy; $E = k + E_k$.

If the variation of form factors with momentum transfer is neglected, the contributions from Fig. 1 are

$$\text{Reg}_3 = -2\Lambda(1-y) \quad g_5 = \Lambda \quad g_6 = -\Lambda,$$

where

$$\Lambda = \frac{1}{2\mu E_k} \left(\frac{1-g^2}{\mu\tau} \right)^{\frac{1}{2}} \frac{4\pi}{y_0 - y}; \quad y_0 = 1 + \frac{\mu^2}{2k^2}.$$

With assumption (a), discussed in the main body of this paper, and omitting π^0 decay effects, the real parts of the g_i may be found from Table III. The correspond-

¹² It is interesting to observe that the effect on neutron Compton scattering should be even more pronounced, since the Klein-Nishina amplitude is absent. However, neutron scattering can only be inferred from deuteron experimental data, and present theoretical uncertainties in the prediction of deuteron cross section from neutron and proton amplitudes appear to nullify whatever advantage the increased neutron effect might bring. See R. H. Capps, *Phys. Rev.* **106**, 1031 (1957).

¹³ L. G. Hyman *et al.*, *Phys. Rev. Letters* **3**, 93 (1959).

TABLE III. Real parts of amplitudes with assumption (a).

K_L (Mev)	$\text{Re } f_1$	$\text{Re } f_2$	$\text{Re } f_3$	$\text{Re } f_4$	$\text{Re } f_5$	$\text{Re } f_6$
0	1.000	0	0	0	0	0
50	0.984-0.030 y	-0.021	0.120-0.199 y	-0.199	-0.199	0.071
100	0.922-0.128 y	+0.031	0.252-0.397 y	-0.397	-0.397	0.136
140	0.796-0.286 y	0.155	0.418-0.571 y	-0.571	-0.571	0.183
190	0.582-0.704 y	0.533	0.669-0.884 y	-0.884	-0.884	0.239
230	0.756-1.238 y	1.037	0.518-1.222 y	-1.222	-1.222	0.281
270	1.106-1.630 y	1.401	0.179-1.475 y	-1.475	-1.475	0.321

TABLE IV. Real parts of amplitudes with assumption (b).

K_L (Mev)	$\text{Re } f_1$	$\text{Re } f_2$	$\text{Re } f_3$	$\text{Re } f_4$	$\text{Re } f_5$	$\text{Re } f_6$
0	1.000	0	0	0	0	0
50	0.980-0.026 y	-0.025	0.118-0.199 y	-0.199	-0.199	0.071
100	0.906-0.112 y	+0.015	0.244-0.396 y	-0.396	-0.396	0.136
140	0.764-0.254 y	0.123	0.398-0.569 y	-0.569	-0.569	0.183
190	0.522-0.642 y	0.471	0.613-0.878 y	-0.878	-0.878	0.239
230	0.662-1.144 y	0.943	0.410-1.210 y	-1.210	-1.210	0.281
270	0.972-1.496 y	1.267	-0.003-1.455 y	-1.455	-1.455	0.321

TABLE V. Imaginary parts of amplitudes.

K_L (Mev)	$\text{Im } g_1$	$\text{Im } f_2$	$\text{Im } f_3$	$\text{Im } f_4$	$\text{Im } f_5$	$\text{Im } f_6$
190	-0.366-0.078 y	0.078	0.366-0.039 y	-0.039	-0.039	0
230	-0.716-0.441 y	0.441	0.716-0.221 y	-0.221	-0.221	0
270	-0.748-1.719 y	1.719	0.748-0.860 y	-0.860	-0.860	0

ing quantities based on assumption (b) are given in Table IV. The imaginary parts of the g_i (with either assumption) may be found from Table V. In all these

tables, the functions whose real or imaginary parts are given actually $f_i \equiv (2kM/c^2)g_i$. The left-hand column gives the laboratory photon energy in Mev.